Journal of Nanoparticle Research (2007) 9:427–440
DOI 10.1007/s11051-006-9086-5

Research Paper

Photochemical synthesis of ZnO/Ag nanocomposites

V. V. Shvalagin, A. L. Stroyuk* and S. Ya. Kuchmii
*Pisarzhevski Institute of Physical Chemistry, National academy of sciences of Ukraine, 31 Nauki av., 03028, Kiev, Ukraine; *Author for correspondence (Tel.: +38-044-525-0270; Fax: +38-044-525-6662; E-mail: stroyuk@inphyschem-nas.kiev.ua/photochem@ukrpost.net)*

Received 28 September 2005; accepted in revised form 10 February 2006

Key words: semiconductor photocatalysis, ZnO nanoparticles, silver nanoparticles, Mie theory, metal-semiconductor composites, plasmon resonance, sensitization, methylene blue

Abstract

Composite ZnO/Ag nanoparticles have been formed via the photocatalytic reduction of silver nitrate over the ZnO nanocrystals, their optical, electrophysical and photochemical properties have been investigated. Mie theory has been applied to analyze the structure of the absorption spectra of ZnO/Ag nanocomposite. The irradiation effects upon the optical properties of ZnO/Ag nanostructure have been investigated. It has been found that the irradiation of ZnO/Ag nanoparticles results in electrons accumulation by both the semiconductor and the metallic components of the nanocomposite. It has been found that silver nitrate can be photochemically deposited onto the surface of ZnO nanoparticles under the illumination with the visible light in the presence of the sensitizer – methylene blue. Kinetics of the sensitized Ag(I) photoredution has been studied. It has been concluded that the key stage of this process is the electron injection from singlet-excited methylene blue molecule into ZnO nanoparticle.

Introduction

Nanometer semiconductor particles attract today great attention due to their unusual electronic and photophysical properties, differing drastically from the properties of bulk (micrometer) crystals of the same chemical composition (Henglein, 1997; Khairutdinov, 1998; Stroyuk et al., 2005a). There are many various methods of the preparation of metal and semiconductor nanoparticles, while the synthetic approaches to metal-semiconductor nanostructures remain still under development.

Among the possible ways to these structures there is one very promising preparative technique exploiting the ability of some semiconductors (CdS, ZnO, TiO_2 etc.) to catalyze photochemical reduction of Pt(IV), Au(I, III), Ag(I), Cu(I), Pb(II), Cd(II) and other metals (Kulak, 1986; Beydoun et al., 1999; Kryukov et al., 2000; Wood et al., 2001). Photochemical synthesis of metal-semiconductor nanostructures has several advantages over other synthetic techniques, such as chemical and electrochemical metal deposition, electrostatical coupling between metal and semiconductor nanoparticles, metal sputtering etc. These are comparatively mild synthesis conditions, favourable prerequisites for the formation of tight electronic contact between the components, well controllable kinetics of photodeposition and others. It is evident though, that photocatalytic synthesis of metal-semiconductor nanostructures can be carried out only in case of photochemically active semiconductors (TiO_2, ZnO, CdS, SnO_2,

ZnS etc.). Most of them have comparatively wide band gaps ($E_g > 2.2$ eV) and therefore are inherently insensitive to the visible light. This limitation can be eliminated via the sensitization of semiconductor nanoparticles with various organic dyes, which can be excited by the visible light and induce at that redox-reactions on the surface of the semiconductor.

Recently we have examined spectral properties of zinc oxide nanoparticles of different size, their photochemical behaviour and photocatalytic activity in the reduction of Cu(II) and Pb(II) compounds, as well as Cu(II)–Ag(I) and Cd(II)–Ag(I) mixtures in alcohol solutions (Stroyuk et al., 2005b).

Here we report on the photocatalytic synthesis of metal-semiconductor ZnO/Ag nanocomposites under the irradiation with mild UV (absorbed by ZnO nanoparticles) and visible (absorbed by a sensitizer) light. We discuss kinetics of silver(I) photoreduction in both cases as well as the evolution of spectral properties of ZnO/Ag nanoparticles in the course of the irradiation.

Experimental

Colloidal ZnO solutions (with molar concentrations 1×10^{-3}–2×10^{-3} M) have been prepared via hydrolysis of $Zn(CH_3COO)_2$ (reagent grade) in the presence of NaOH (pure) in twice-distilled dry 2-propanol at 0–5°C (Bahnemann et al., 1987; Wood et al., 2001; Pesika et al., 2003). In typical procedure an amount of dry zinc acetate (0.0915 g, 0.5 mmol) has been dissolved at continuous refluxing in 60 ml of twice-distilled 2-propanol at 50–60°C. Resulting solution has been diluted to 230 ml by 2-propanol and cooled to 0°C. Sodium hydroxide powder (0.032 g, 0.8 mmol) has been dissolved in 20 ml of twice distilled 2-propanol at 50–60°C and then cooled to 0°C. Alcoholic solutions of sodium hydroxide and zinc acetate have been then mixed dropwise at intense stirring at 0°C. After the synthesis colloidal ZnO solution has been heated at 55–60°C for 2 h, cooled and stored in the dark at 5–10°C.

To prepare samples for XRD studies, ZnO nanoparticles have been precipitated from alcoholic solution by water. To 50 ml of colloidal solution 10 ml of water have been added, the solution has been kept at room temperature overnight. The precipitate has been separated from the solution, washed two times with water, two times with diethyl ether and dried at room temperature. X-rays diffraction spectra have been recorded on DRON-3M type diffractometer using copper $K\alpha$ irradiation.

Agglomeration number of ZnO nanoparticles (N_{ZnO}) has been calculated as

$$N_{ZnO} = \frac{4}{3}\pi R^3 \rho N_a M^{-1},$$

where R is ZnO nanoparticles radius, ρ is the density of bulk zinc oxide (5.47×10^3 kg m^{-3}), N_a is the Avogadro constant, M is the ZnO molecular mass.

Silver nitrate (Aldrich) and methylene blue (MB) have been used without additional purification. Solutions, containing colloidal zinc oxide (5×10^{-4}–2×10^{-3} M), silver nitrate (2×10^{-5}–1×10^{-4} M) and MB (5×10^{-6} – 5×10^{-5} M), have been prepared from stock 2×10^{-3} M ZnO, 5×10^{-2} M $AgNO_3$ and 1×10^{-3} M MB solutions in 2-propanol.

The irradiation of solutions has been carried out using filter-cut 310–390 nm light segment of 1000 W high-pressure mercury lamp or 500 W incandescent lamp in glass 1.0 cm cuvettes. Five centimeter water filter has been placed between the light source and the work cuvette to reduce heating of reacting mixtures. Oxygen has been removed from the cuvettes before the experiments via continuous argon bubbling.

Results and discussion

Structural, optical and photochemical properties of ZnO nanoparticles

Fundamental absorption band edge of freshly prepared ZnO colloid (λ_{tr}) is located at 310–315 nm. Pronounced hypsochromic shift of the edge of the absorption band of ZnO nanoparticles from the position, typical for bulk zinc oxide ($\lambda_{tr} = 390$ nm), indicates that ZnO nanoparticles are in quantum confinement regime (Bahnemann et al., 1987; Wood et al., 2001). Ageing of the freshly prepared ZnO colloid at 55–60°C for 2 h results in the bathochromic shift of λ_{tr} to 350–355 nm and substantial increase in the stability of the sols towards aggregation.

Band gap of ZnO nanoparticles (E_g) has been calculated as the energy, corresponding to the wavelength of the cross point between the abscissa axis and the tangent to the long-wave edge of the absorption band of ZnO colloids. From the average value $E_g = 3.55$ eV the size of ZnO nanoparticles has been estimated to be $2R = 5.0$ nm using the effective masses approximation in the form of the Equation (1) (Wang & Herron, 1991; Henglein, 1997; Khairutdinov, 1998).

$$\Delta E_g = \frac{\hbar^2 \pi^2}{2R^2}\left(\frac{1}{m_e^* m_0} + \frac{1}{m_h^* m_0}\right) \quad (1)$$

where ΔE_g is the odds between E_g of colloidal and bulk zinc oxide (for bulk ZnO $E_g^{bulk} = 3.2$ eV (Bahnemann et al., 1987), $\hbar$ – reduced Planck constant, m_e^*, m_h^* are the effective masses of conduction band electrons and valence band holes respectively (for ZnO $m_e^* = 0.25, m_h^* = 0.59$ (Shim & Guyot-Sionnest, 2001; Wong et al., 2001)), m_0, e are the rest mass and the charge of electron.

XRD spectrum of precipitated ZnO nanoparticles (Figure 1a) shows broadened maxima, typical for hexagonal zincite (Wong et al., 2001; Tani et al., 2002). Scherer equation has been used to calculate the average size of ZnO nanocrystallites, which has been found to be 5.0 ± 0.2 nm. This value coresonds perfectly to $2R$, calculated from the absorption spectra in effective masses approximation.

It has been found that the irradiation of deaerated ZnO colloids induces reversible hypsochromic shift of λ_{tr} (Figure 1b). The edge of the absorption band of irradiated ZnO solution returns quickly to initial position, when air is admitted to the cuvette. In deaerated solutions, where no electron acceptor (such as oxygen) is present, the magnitude of $\Delta\lambda_{tr}$ remains unchanged for several days. It is known that such dynamic photochemical shift of the band edge of semiconductor nanocrystals originates from dynamic Burstein–Moss effect – the growth of the first excitonic transition energy due to the population of the lowest electronic states near the conduction band edge by excessive electrons (Albery, 1985; Kamat et al., 1989; Liu & Bard, 1989; Wood et al., 2001). Fast capture of valence band holes by alcohol molecules, surrounding the surface of nanocrystals, promotes strongly this process:

$$ZnO + h\nu \rightarrow ZnO\left(e_{CB}^- + h_{VB}^+\right) \quad (2)$$

$$h_{VB}^+ + (CH_3)_2CHOH \rightarrow \left\{(CH_3)_2CH^{\bullet +}OH\right\} \rightarrow H^+ + (CH_3)_2C^{\bullet}OH \quad (3)$$

$$e_{CB}^- + []_{surf} \rightarrow e_{tr}^- \quad (4)$$

where $h\nu$ is a light quantum; e_{CB}^-, h_{VB}^+ are conduction band electron and valence band hole, $[]_{surf}$ is the surface trap, e_{tr}^- is the electron trapped on surface lattice defects and adsorbed Zn(II) species.

The wavelength shift $\Delta\lambda_{tr}$ (and corresponding energy shift ΔE_B) can be calculated as the width of the bleaching band, forming in differential spectrum of irradiated solution (Figure 1c), measured on the half-height of the band in the maximum. ΔE_B depends on the density of excessive electrons, accumulated by ZnO nanoparticles (n_e) [1–3]:

$$\Delta E_B = \left[1 + \frac{m_e^*}{m_h^*}\right] \times \left[\frac{h^2}{2m_e^*} \cdot \left(\frac{3n_e}{8\pi}\right)^{\frac{2}{3}} - 4kT\right] \quad (5)$$

where k is Boltzmann constant, T – temperature (K). It can be shown that $\Delta E_B = 0.19$ eV corresponds to approximately 4–5 excessive electrons per one ZnO nanoparticle.

Formation and optical properties of ZnO/Ag nanostructures

Irradiation of ZnO solution in the presence of silver nitrate results in the formation of new intense absorption band, centered at 390–430 nm (Figure 2a, curves 1–6). According to (Doremus, 1965; Henglein, 1993; Pileni, 1998; Stenzel, 1999), such absorption bands belong to small (1–100 nm) particles of metallic silver. They originate from the excitation of collective resonance oscillation of the electron gas within the near-surface layer of metal nanoparticles and are referred to as surface plasmon resonance (SPR) absorption bands. So, it can be concluded that the irradiation of ZnO nanoparticles in the presence of silver nitrate results in the reduction of Ag(I) and formation of ultrasmall silver particles. The intensity of silver SPR band depends on the concentration of silver nitrate and at $[Ag(I)] = 1\times10^{-5} - 1\times10^{-4}$ M after completion

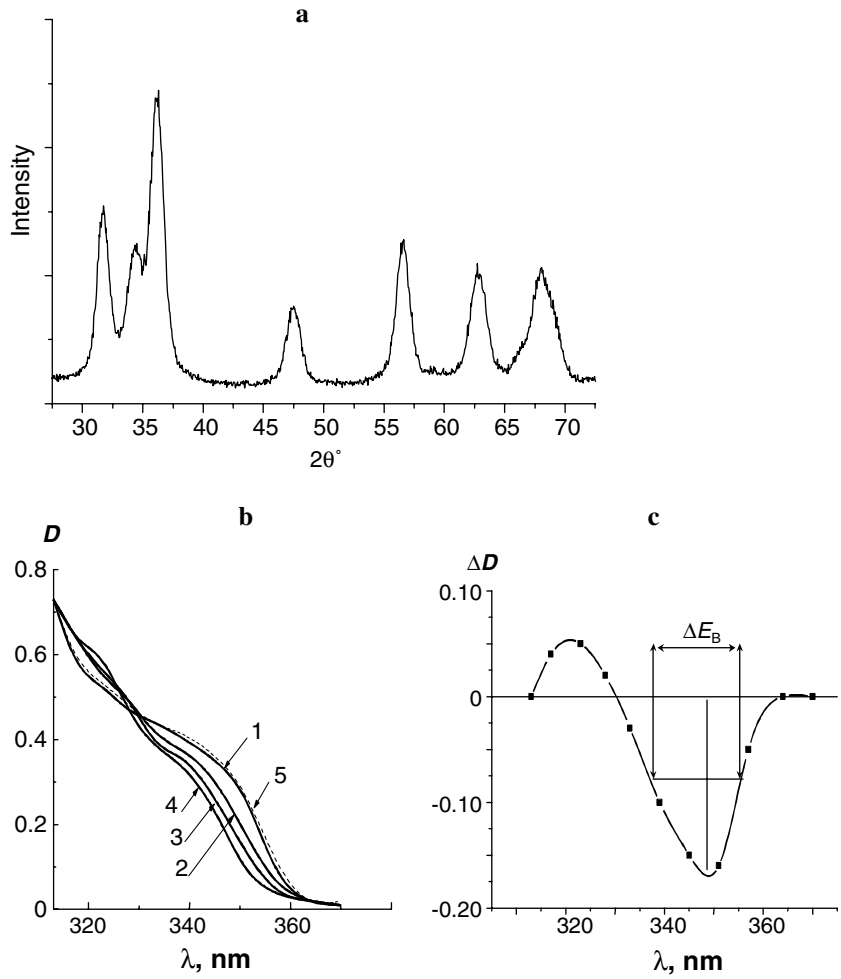

Figure 1. (a) X-rays diffraction spectrum of ZnO nanoparticles. (b) Absorption spectra of colloidal ZnO solution in 2-propanol before the irradiation (1), after the irradiation during 10 (2), 20 (3) and 30 min (4), after the admission of the air to the irradiated solution (5). (c) Differential absorption spectrum of colloidal ZnO solution in 2-propanol plotted via the subtraction of the spectral curves (1) and (4) from Figure 1b. Light intensity $I = 3\times10^{-6}$ Einstein min^{-1}, $[ZnO] = 2\times10^{-3}$ M, cuvette length $l = 1.0$ cm.

of the photochemical reaction obeys Lambert–Beer law, molar extinction coefficient in the maximum of the band being $(13.5 \pm 0.5)\times10^3$ $M^{-1} \times cm^{-1}$.

Before the analysis of the optical properties of ZnO/Ag nanocomposite, we can make some preliminary estimation of the size of photodeposited silver nanoparticles as well as the size of ZnO/Ag nanocomposite. Three assumptions may be made to facilitate these estimations. First, we assume zinc oxide nanoparticles to be monodisperse, their diameter being equal to 5.0 nm; (2) the surface of ZnO nanocrystals is homogeneous and therefore equal amount of silver ions are adsorbed by each semiconductor nanoparticle; (3) only one (spherical) silver particle forms during the photocatalytic process on each ZnO nanocrystal. First assumption is based on the results of the TEM studies of ZnO nanoparticles, synthesized in 2-propanol (Bahnemann et al., 1987), revealing on the relatively narrow, about 20% (5.0 ± 0.5 nm), size distribution of ZnO nanocrystals, synthesized in 2-propanol. Steep fall of absorption edge as well as the presence of distinct excitonic shoulder in the

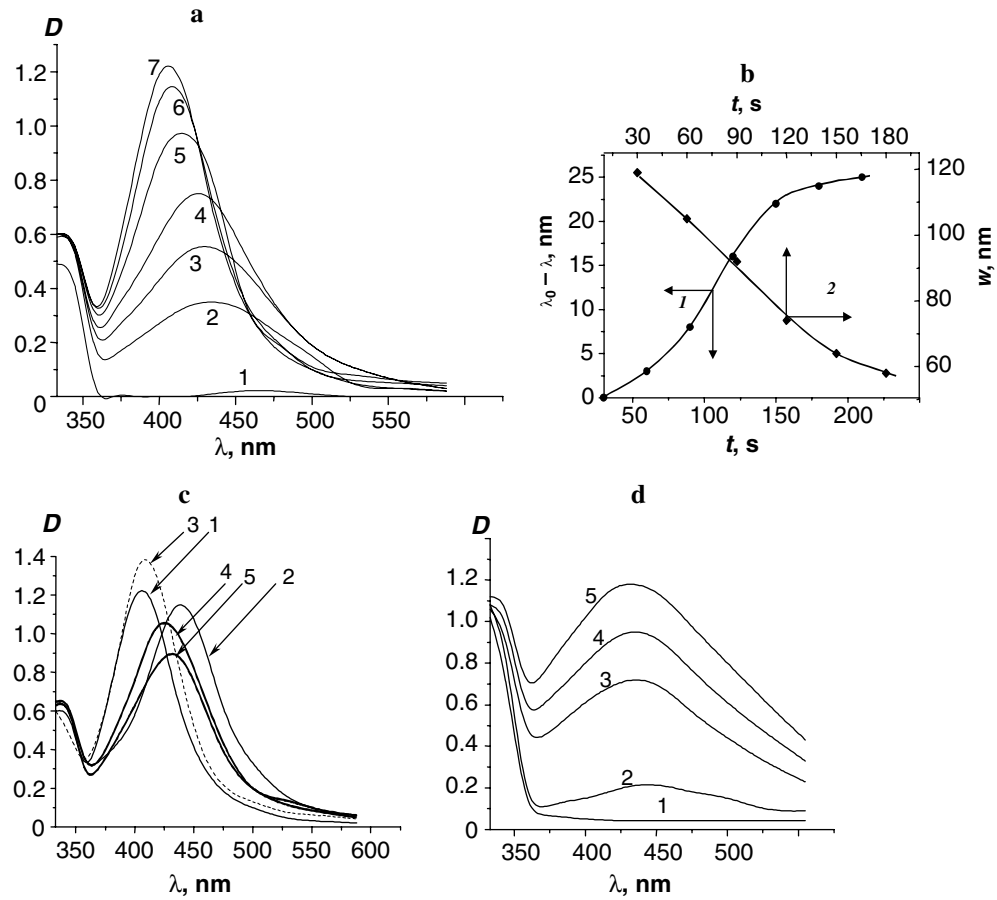

Figure 2. (a) Absorption spectra of deaerated colloidal ZnO solution, containing $AgNO_3$, before the irradiation (1), after the exposure for 30 (2), 60 (3), 90 (4), 120 (5), 150 (6) and 510 s (7). (b) The correlation between the magnitude of hypsochromic shift ($\lambda_0 - \lambda$) of the maximum of silver SPR band relative to $\lambda_0 = 428$ nm and exposure t (1); the correlation between the change of the width of silver SPR band, measured at half-height in the maximum, and t (2). (c) Evolution of the position and the intensity of silver SPR band at the storage of ZnO/Ag solution in the dark, subsequent irradiation and after air admission to pre-irradiated ZnO/Ag solution. Curve 1 corresponds to the curve 7 from the Figure 1a; curve 2 corresponds to the absorption spectrum of the solution (1) aged in the dark during 16 h; curve (3) is the absorption spectrum (2) after the irradiation in the absence of oxygen during 600 s; curve (4) is the spectrum of the solution (3) after the admission of air; curve (5) is the spectrum of air-saturated solution (4) after 2 h storage in the dark. (d) Absorption spectra of air-saturated 2-propanolic solution, containing ZnO nanoparticles, and $AgNO_3$ before the irradiation (1) and after the exposure for 2 (2), 10 (3), 15 (4) and 20 min (5). $[ZnO] = 1 \times 10^{-3}$ M, $[AgNO_3] = 7.5 \times 10^{-5}$ M, light intensity $I = 3.0 \times 10^{-6}$ Einstein min^{-1}, cuvette length $l = 1.0$ cm.

absorption spectra of ZnO nanoparticles also indicates on the narrow size distribution of semiconductor nanocrystals. Second assumption is used to facilitate the estimations and ignores real statistical distribution of silver ions between the ZnO nanoparticles. Finally, third assumption is based on our results, presented here below, about the autocatalytic character of silver photoreduction on the surface of ZnO nanocrystals. The ability of metallic silver to catalyze further reduction of Ag(I) may apparently create conditions for the nucleation and growth of only one metal particle per each semiconductor nanocrystal. Using these assumptions we may suppose that ZnO nanoparticles act as a template, determining the average size of forming silver nanoparticles. It can be easily calculated that about 200 Ag(I) species can be reduced on the surface of each

5.0 nm ZnO nanoparticle at $[ZnO] = 1 \times 10^{-3}$ M and $[Ag(I)] = 7.5 \times 10^{-5}$ M. Since Ag(I) reduction is equiprobable on the surface of each semiconductor nanocrystal, we may assume that silver nanoparticles formed on the surface of ZnO nanocrystals will consist of 200 silver atoms on average. Assuming then that the densities of nanoparticulate and bulk silver are the same, we can show, that the average radius of Ag^0 nanoparticles is close to 0.8–0.9 nm. Therefore, the size of composite ZnO/Ag particles, if we assume it to be equal to the doubled sum of the radii of spherical ZnO and Ag^0 particles, will then be 6.5–7.0 nm. It should be noted, that this figure should be treated only as rough estimation. Disperse silver is oxidized, when exposed to air, so we could not perform direct determinations of the size of Ag^0 nanoparticles.

Below we give the equations, necessary for the analysis of the optical properties of silver nanoparticles, forming at the photocatalytic reduction of $AgNO_3$. Mie theory gives the following expression for the absorption coefficient $\alpha(\lambda)$ of small metal nanoparticles (see, for example, Doremus, 1965; Henglein, 1993; Pileni, 1998):

$$\alpha = \frac{18\pi}{\ln 10} \cdot \frac{10^5}{\lambda} \cdot \frac{\mathrm{M} n_0^3}{\rho} \cdot \frac{\varepsilon_2}{\left(\varepsilon_1 + 2n_0^2\right)^2 + \varepsilon_2^2} \tag{6}$$

where M and ρ are the molar mass and the density of the metal, n_0 is the refraction index of dispersive medium, λ is the wavelength, ε_1, ε_2 are real and imaginary components of the complex dielectric function of the metal $\varepsilon(\lambda)$.

Wavelength-dependent parameters ε_1 and ε_2 characterize light dispersion and absorption respectively. When the size of metal nanoparticles is smaller than the length of electron free path R_e (52 nm for silver (Doremus, 1965; Henglein, 1993)), a function of nanoparticle radius $\varepsilon_2'(R)$ should be used instead of ε_2:

$$\varepsilon_2' = \varepsilon_2 + \gamma \frac{\varpi_P^2 \lambda^3 \mathrm{V_F}}{(2\pi c)^3 R_e} \tag{7}$$

where γ is the coefficient of SPR band deformation under the influence of adsorbed substrates (according to (Skillman, 1968; Henglein, 1993), for Ag nanoparticles typical values γ are 0.5–0.6), ω_p is the plasmon frequency of a metal (for silver $\omega = 1.4 \times 10^{16}$ s^{-1} (Doremus, 1965; Henglein, 1993)), V_F is the velocity of electron on Fermi level (for silver $V_F = 1.4 \times 10^6$ m s^{-1} (Henglein, 1993)), c is the light velocity in the vacuum, R_e is the radius of the domain of free electron motion (assumed to be equal to R when $R < R_e$).

Position of SPR band maximum (λ_{max}) depends on dielectric properties of the metal and the solvent as well as on the density of free electrons (Doremus, 1965; Henglein, 1993; Pileni, 1998):

$$\lambda_{max}^2 = \frac{(2\pi c)^2 m_e \left(\varepsilon_0 + 2n_0^2\right)}{4\pi e^2 N_e} \tag{8}$$

where N_e is the electrons density of metal nanoparticles (for bulk silver $N_e = 5.8 \times 10^{28}$ m^{-3} (Pileni, 1998)), ε_0 – wavelength-independent component of the dielectric permeability of the metal.

Half-width of SPR band, measured at the half of its height in the maximum (w), is informative parameter, characterizing metal nanoparticles. It depends on the radius of metal nanoparticles and N_e (Doremus, 1965; Henglein, 1993; Pileni, 1998):

$$w = \frac{\left(\varepsilon_0 + 2n_0^2\right) c m_e \mathrm{V_F}}{2 N_e e^2 R} \tag{9}$$

Equation (10) gives the average number of free electrons per particle:

$$n_{fe} = N_e \cdot \frac{4\pi R^3}{3} \tag{10}$$

It has been found that theoretical position of the maximum of silver SPR band in 2-propanol ($\lambda_{max} = 390$ nm) calculated with the Equation (6), does not match to experimental results ($\lambda_{max} = 405 - 430$ nm, Figure 2a). It should be remembered, however, that the silver is deposited in microheterogeneous medium on the interface between zinc oxide and the alcohol. Forming silver nanoparticles should therefore have close contact with the surface of ZnO nanoparticles and their electronic properties could be affected not only by the dispersive medium, but also by the electronic system of the semiconductor. We have tried to take these interactions into account, using for the calculations apparent refraction index n_0', which is the average between the refractions of 2-propanol ($n_0 = 1.324$) and zinc oxide ($n_0 = 2.029$): $n_0' = (1.324 + 2.029)/2 = 1.536$.

The size of silver nanoparticles should also be taken into consideration. Using ε_2', calculated with the expression (7), and taking $2R$ to be equal to 6.5 nm, we have obtained $\lambda_{max} = 425$ nm and molar extinction coefficient $\varepsilon_{425} = 1.8 \times 10^4$ M^{-1} cm^{-1}. These values are close to experimentally observed parameters ($\lambda_{max} = 428$ nm, $\varepsilon_{428} = 1.4 \times 10^{-4}$ M^{-1} cm^{-1}).

Continuous hypsochromic shift of the maximum of SPR band (Figure 2b, curve 1) and some decrease of w (Figure 2b, curve 2) have been observed during the irradiation of ZnO–$AgNO_3$ systems. Examination of expressions (8) and (9) indicates that the hypsochromic shift $\Delta\lambda = \lambda_0 - \lambda$ (where λ_0 and λ are initial and current positions of the maximum of silver SPR band) and the decrease of w can originate from an increase in the density of free electrons of growing silver nanoparticles. This suggestion is confirmed by several experimental observations: (i) the shift of the maximum of SPR band has not been observed in the presence of oxygen, capable to accept photogenerated ZnO conduction band electrons; (ii) instant reverse bathochromic shift of the maximum of SPR band has been observed upon the admission of the air into the irradiated cuvette (Figure 2c); (iii) slow reverse bathochromic shift of the maximum of SPR band has been observed at prolonged storage of the irradiated solutions in the dark; (iv) hypsochromic shifts both of the maximum of plasmon band and that of the edge of fundamental absorption band of ZnO nanoparticles have been observed again upon resuming the irradiation of the solutions after prolonged storage in the dark (Figure 2c, curve 9).

It can be derived from Equations (8) and (9) that $\Delta\lambda = 25$ nm corresponds to the accumulation of 4 excessive electrons on average per each ZnO/Ag particle (Δn_{ef}, see Table 1). The mechanism of the accumulation of excessive charge in this case does not apparently differ from that, discussed above for individual ZnO nanoparticles (see reactions 2, 3).

Close contact between the semiconductor and the metal, composing ZnO/Ag nanoparticles, result apparently in substantial overlapping of the wave functions of electron gas of silver nanoparticle and the conduction band of zinc oxide (Wood et al., 2001). The size of a domain of electron confinement in metal nanoparticles ($2R_e$) can be estimated with the use of expression (9) and the values of w at different stages of the photochemical reaction (see Figure 2a and Table 1). It has been found that the formation of ZnO/Ag nanocomposite is accompanied by gradual growth of $2R_e$. After complete reduction of Ag(I) $2R_e = 5.5$ nm (Table 1). This value exceeds substantially the size of Ag^0 nanoparticles and approaches to the estimated above diameter of composite ZnO/Ag nanoparticles (6.5–7.0 nm).

Photocatalytic reduction of Ag(I) has been also observed in air-saturated solutions (Figure 2d). In this case the position of the maximum of silver SPR band remains constant during the irradiation. The rate of photoreduction in air-saturated solutions is substantially lower in the comparison with deaerated solutions due to partial withdrawal of photogenerated electrons by molecular oxygen or due to partial oxidation of ultradisperse silver by oxygen. The possibility of the latter process is confirmed by gradual decrease of SPR absorbance at the storage of air-saturated ZnO/Ag colloids in the dark. It has been found that SPR bands of silver nanoparticles, formed at the photoreduction

Table 1. Evolution of some characteristics of ZnO/Ag nanocomposite in the course of the irradiation of ZnO colloid in the presence of $AgNO_3$

t, s	λ_{max}, nm	w, nm	$\Delta N_e \times 10^{-28}$, m^{-3}	Δn_{fe}	$2R_e$, nm	ΔE_F, eV
30	428	119	0.03	0.3	2.2	0.03
60	425	105	0.09	1.0	2.4	0.07
90	422	92	0.19	2.0	2.8	0.13
120	411	70	0.51	3.0	4.2	0.33
150	405	64	0.70	4.0	4.5	0.45
510	403	58	0.78	4.0	5.5	0.50

Notes: t is the duration of the irradiation, ΔN_e is the excess of electronic density accumulated on growing ZnO/Ag nanoparticles at the irradiation, Δn_{fe} is the number of free electrons, accumulated by each composite ZnO/Ag nanoparticle, ΔE_F is the increase in Fermi energy of silver nanoparticles.

of Ag(I) in aerated solutions, have greater half-widths w as compared with plasmon bands of silver nanoparticles, synthesized in anaerobic conditions. This w increase can be caused by silver oxide formation or oxygen adsorption on the surface of silver nanoparticles (Henglein, 1998). Oxygen molecules can accept electronic density from Ag^0 and reduce N_e, broadening in that way SPR band.

The accumulation of the excess of electrons by ZnO/Ag nanoparticles results in the change of collective Fermi energy of the composite system. Since the capacity of silver is of an order of magnitude greater than that of zinc oxide, collective Fermi level of the nanocomposite depends predominantly on the density of free electrons of silver nanoparticles N_e:

$$E_F = 1.6 \times 10^{-19} \cdot \frac{h^2}{8m_e} \cdot \left(\frac{3N_e}{\pi}\right)^{\frac{2}{3}} \qquad (11)$$

where E_F is the Fermi energy (for bulk silver $E_F = 5.48$ eV (Henglein, 1993).

It has been found that the accumulation of electrons by ZnO/Ag nanoparticles actually results in the growth of the Fermi energy of silver nanoparticles (Table 1). The maximal increase in E_F is about 0.5 eV. The Fermi level of non-degenerate zinc oxide is located in the band gap, but the accumulation of excessive electron shifts it into the conduction band of the semiconductor. The potential of the edge of ZnO conduction band in neutral media is close to −0.7 V versus NHE (Wood et al., 2001). The Fermi level of non-polarized silver electrode is −0.15 V versus NHE (Moelwyn-Hughes, 1961). So, we have concluded that the accumulation of excessive charge by ZnO/Ag nanoparticles results in the equilibration between Fermi level of ZnO/Ag nanocomposite and ZnO conduction band edge. Similar phenomena have been also observed in other ZnO-based nanostructured systems, such as ZnO/Ag, ZnO/Cu (Wood et al., 2001), ZnO/Au (Wood et al., 2001; Subramanian et al., 2003), TiO_2/Au (Kamat, 2002) and TiO_2/Ag (Cozzoli et al., 2004).

Kinetics of the photochemical formation of ZnO/Ag nanocomposite

Table 2 illustrates the influence of various parameters of the reaction system on quantum efficiency of photocatalytic Ag(I) reduction. Quantum yields of this process (γ_{Ag}) are quite high. In certain cases $\gamma_{Ag} = 0.5$ (Table 2), i.e. is comparable with quantum yields of silver formation in photographic emulsions based on silver halogenides (James, 1977). It can be seen from the Table 2, that quantum efficiency of Ag(I) photoreduction grows at the deaeration of a solution, an increase in silver and ZnO concentrations as well as light intensity (I). High quantum yields of the photoreduction coupled with the linearity of the correlation between the quantum yield and the light intensity indicate that this photoprocess competes efficiently with electron-hole recombination in ZnO nanocrystals.

Figure 3a shows typical kinetic curve of photocatalytic Ag^0 deposition. Initial section of the curve (see the inset in Figure 3a) is S-shaped, which is peculiar for autocatalytic processes. We have assumed that autocatalytic photoreduction of Ag(I) on the surface of ZnO nanoparticles may be described by the following scheme:

$$ZnO + h\nu \rightarrow ZnO\left(e^-_{CB} + h^+_{VB}\right)$$

Table 2. The quantum yields (γ_{Ag}) of photocatalytic $AgNO_3$ reduction.

$[AgNO_3] \times 10^4$, M	$[ZnO] \times 10^3$, M	Deaeration	γ_{Ag}
0.5	2.0	+	0.14
1.0	2.0	+	0.32
2.0	2.0	+	0.60
0.5	2.0	−	0.04
1.5	2.0	−	0.19
2.5	2.0	−	0.31
1.0	0.5	+	0.11
1.0	1.0	+	0.21
1.0	2.0	+	0.31
2.5	0.5	−	0.11
2.5	1.0	−	0.15
2.5	2.0	−	0.30
2.0[(a)]	2.0	+	0.49
2.0[(b)]	2.0	+	0.62
2.0	2.0	+	0.59
1.0[(a)]	2.0	−	0.30
1.0[(b)]	2.0	−	0.24
1.0	2.0	−	0.15
2.5[(c1)]	2.0	−	0.37
2.5[(c2)]	2.0	−	0.47

Notes: In cases [(a)] and [(b)] light intensity I is 0.63×10^{-7} and 1.25×10^{-7} einstein min^{-1} respectively, in other cases $I = 2.5 \times 10^{-7}$ einstein min^{-1}; [(c)] – in the presence of $[H_2O] = 0.1$ M[(c1)], 0.25 M[(c2)].

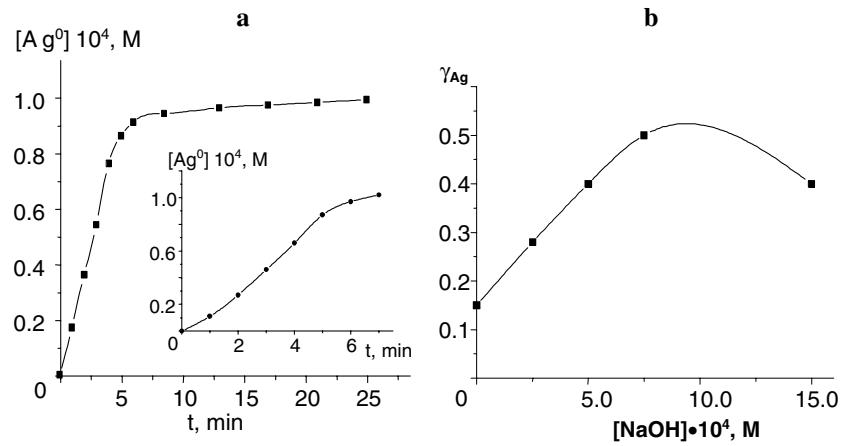

Figure 3. (a) Growth of the intensity of silver SPR band at $\lambda = 430$ nm in deaerated solutions. *Inset*: the fragment of the kinetic curve of Ag^0 deposition corresponding to the initial stage of the irradiation. (b) The correlation between the quantum yield of silver photoreduction (γ_{Ag}) and NaOH concentration. Light intensity $I = 3.0\times10^{-6}$ Einstein min^{-1}. [ZnO] $= 2\times10^{-3}$ M, $[AgNO_3] = 7.5 \times 10^{-5}$ M.

$$h^+_{VB} + (CH_3)_2CHOH \rightarrow (CH_3)_2C^{\bullet}OH + H^+$$

$$h^+_{VB} + e^-_{CB} \rightarrow h\nu_{lum} + \Delta H \qquad (12)$$

$$e^-_{CB} \rightarrow e^-_{tr} \qquad (13)$$

$$2Ag^+ + ZnO(e^-_{tr}) \rightarrow ZnO/Ag^+_2 \qquad (14)$$

$$ZnO/Ag^+_2 + ZnO(e^-_{tr}) \rightarrow ZnO/Ag_2 \rightarrow \ldots \rightarrow ZnO/Ag_n \qquad (15)$$

$$ZnO(e^-_{tr}, e^-_{CB})/Ag_n \rightarrow ZnO/Ag^-_n \qquad (16)$$

$$ZnO/Ag^-_n + Ag^+ \rightarrow ZnO/Ag_{n+1} \text{and so on} \qquad (17)$$

where $h\nu_{lum}$ is the luminescence quantum, ΔH is the heat, e^-_{tr} is the electron captured in the surface trap, Ag_n is the growing silver cluster.

According to the scheme, Ag(I) is reduced first by photogenerated ZnO conduction band electrons (reactions 13–14), then – by the electrons accumulated by composite ZnO/Ag nanoparticles. Redox-potential of the couple $Ag(I)/Ag^0_{atom}$ is −1.8 V versus NHE (Henglein, 1993). Hence, ZnO conduction band electrons have insufficient potential for the conversion of Ag(I) into Ag^0_{atom}. It should be take into account, however, that only adsorbed Ag(I) species compete efficiently with recombination processes and capture photogenerated electrons. Saturation of ZnO adsorption layer with Ag(I) promotes initial stages of the photoreduction, when various charged silver clusters can form. The cluster Ag^+_2, for example, forms at the potentials close to zero (Henglein, 1993).

The photoreduction rate increases upon addition of water to a reacting mixture (Table 2). Similar effect has also the addition of NaOH (Figure 3b). Water increases the extent of sodium acetate hydrolysis (CH_3COONa forms as side-product at the synthesis of ZnO nanoparticles). At that the surface of ZnO nanoparticles can acquire additional negative charge due to OH^- adsorption. Increase of the charge of ZnO double electrical layer results in the growth of the potentials of the conduction and valence band of the semiconductor, i.e. in the augmentation of the driving force of the photocatalytic process. Spectral data indicate that some rate decrease at [NaOH] $> 1\times10^{-3}$ M can be caused by partial coagulation of ZnO nanoparticles.

Photocatalytic Ag(I) reduction under the irradiation with the visible light

Spectral sensitivity domain of ZnO nanoparticles is limited to $\lambda < 370$ nm. Our attempts to sensitize ZnO nanocrystals to the visible light have shown

that such dyes as fluoresceine derivatives and rhodamines can reduce Ag(I) even in the absence of the semiconductor with considerable rates. Methylene blue, in contrast to them, has been found to be inactive in this process. At the same time, it has been found that in the presence of this dye, photocatalytic Ag(I) photoreduction can be successfully carried out under the visible light.

Methylene blue (MB) in 2-propanolic solutions with [MB] $= 5\times10^{-6} - 5 \times 10^{-5}$ M has intense absorption band centered at 665 nm (molar extinction coefficient at 665 nm $\varepsilon_{665} \sim 10^5$ M^{-1} cm^{-1}). It has been found that in the conditions of our experiments dye solutions in 2-propanol retain photochemical stability during 1–2 h exposure.

No changes of the dye absorption spectrum of have been observed upon the addition ZnO nanoparticles ($1\times10^{-4} - 2 \times 10^{-3}$ M). Identity of the adsorption spectra of MB both in the absence and in the presence of ZnO nanoparticles indicates that adsorptive interactions between the semiconductor and the dye do not affect substantially the chromophoric system of MB molecule.

The irradiation of deaerated solutions, containing ZnO nanoparticles and MB molecules, with the visible light ($\lambda > 460$ nm) results in fast decay of dye absorbance. The rate of this photoprocess grows at an increase in sodium acetate concentration or upon NaOH addition. Admission of air to irradiated solutions is followed by slow regeneration of MB absorbance at $\lambda_{max} = 665$ nm. Hence, we have concluded that the bleaching of deaerated dye solutions at the irradiation in the presence of ZnO nanocrystals is associated with the formation of *leuco*-MB. It is known, that *leuco*-form of MB does not absorb in the visible domain of the spectrum (Terenin, 1967; Lee & Mills, 2003).

No spectral transformations, indicating the formation of Ag^0, have been observed in the absence of ZnO nanoparticles. On the contrary, synchronous decay of dye absorbance and formation of additional band at 380–550 nm with the maximum at 430–440 nm (Figure 4a) have been observed at the illumination of deaerated MB solutions, containing both silver nitrate and ZnO nanoparticles. Parameters of new absorption band (the shape, position of the maximum, the intensity) are typical for SPR absorption of silver nanoparticles. The rate of MB photoreduction in the presence of Ag(I) is slower as compared with the system ZnO–MB, probably due to competition between Ag^0 deposition and dye reduction. It has been found that both the rate of Ag^0 accumulation and the rate of MB reduction increase upon the addition of sodium hydroxide or sodium acetate. The same, but slower spectral transformations have also been observed in air-saturated solutions (Figure 4b).

Kinetics of sensitized silver photoreduction

The rate of MB-sensitized Ag(I) photoreduction has been measured as the change of silver SPR band intensity at its maximum at small (up to 60 s) exposures. It grows in conditions, favoring to the increase of excited sensitizer concentration, i.e. at

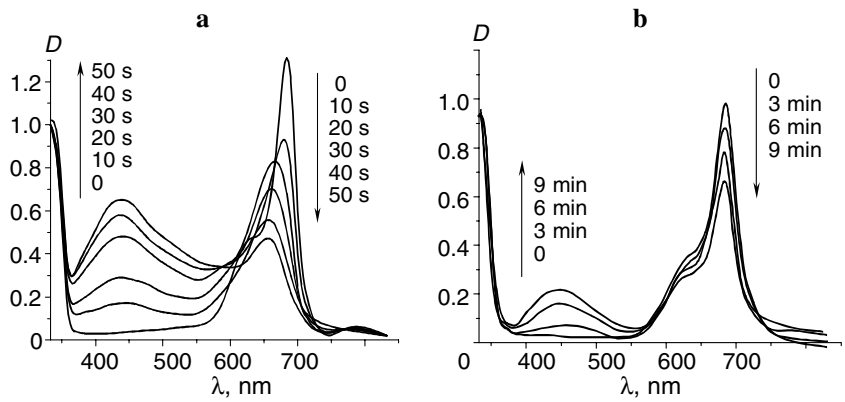

Figure 4. Evolution of the absorption spectrum of the solution, containing ZnO nanoparticles, $AgNO_3$ and methylene blue (MB), at the irradiation in the absence (a) and in the presence of oxygen (b). $[ZnO] = 2 \times 10^{-3}$M, $[AgNO_3] = 1 \times 10^{-4}$ M, $[MB] = 1 \times 10^{-5}$ M.

the increase in the light intensity and dye concentration (Figure 5a), as well as at the deaeration of the solutions. We have assumed that non-linearity of the correlation between the rate of silver photoreduction V and MB concentration $[D]$ (Figure 5a) originates from the saturation of the adsorption layer of ZnO nanoparticles with dye molecules. If we suppose, that MB adsorption is described by Langmuir Equation (17), then linear dependence between V^{-1} and $[D]^{-1}$ should be expected:

$$V = k \cdot [D]_{\text{ads}} = k\frac{K_{\text{ads}}[D]}{1 + K_{ads}[D]} \Rightarrow \frac{1}{V} = \frac{1}{k} + \frac{1}{kK_{\text{ads}}[D]} \quad (18)$$

where k is the rate constant, K_{ads} is the Langmuir constant of dye adsorption on the surface of ZnO nanoparticles, $[D]_{\text{ads}}$ is the surface concentration of MB. Dependences V^{-1}–$[D]^{-1}$ have been actually found to be linear. This fact indicates, that the photoreaction proceeds with the participation of the sensitizer, adsorbed on the surface of ZnO nanoparticles.

The rate of silver photoreduction does not depend on ZnO concentration at $[\text{ZnO}] = 5\times10^{-4}$–$2\times10^{-3}$ M (Figure 5b). Constancy of the rate of Ag(I) photoreduction at different ZnO concentration may be explained by strong adsorption of Ag(I) on the surface of the semiconductor, resulting in the saturation of ZnO adsorption layer with silver. It may be supposed that all silver ions are adsorbed on the surface of the photocatalyst even at $[\text{ZnO}] = 5\times10^{-4}$ M and further increase in the semiconductor concentration does not affect the rate of the photoprocess. On the contrary, an increase in $AgNO_3$ concentration results in linear growth of the rate of silver photoreduction both in aerated and in oxygen-free solutions.

Mechanism of sensitized Ag(I) photoreduction

At the irradiation with the visible light ($\lambda > 460$ nm) MB molecules (D) are excited to the first singlet excited state D^1 with the energy $E^1 = 1.90$ eV. This intermediate is short-lived (0.4 ns (Lee & Mills, 2003)) and converts rapidly into the first triplet excited state D^3($E^3 = 1.45$ eV (Lee & Mills, 2003)). Oxidation potential of MB molecule in the ground state is more positive than +1.0 V versus NHE (James, 1977). We could not find in the literature the exact value of MB oxidation potential, so we have assumed that it is close to well-known oxidation potential of thionine ($E_{\text{ox}} = +1.25$ V versus NHE (Patrick & Kamat, 1992)). So, oxidation potentials of singlet (E^1_{ox}) and triplet (E^3_{ox}) excited MB molecules are close to −0.65 V and −0.2 V versus NHE respectively. Electron injection into the conduction band of 5–6 nm ZnO nanoparticles is possible at potentials more negative than −0.3 V versus NHE (Hoyer & Weller, 1995; Noack et al., 2002). Comparison of

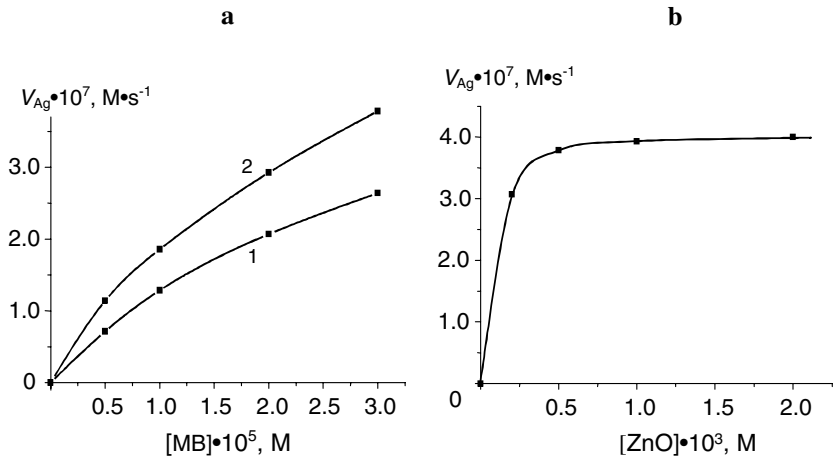

Figure 5. (a) The correlation between the silver photoreduction rate and methylene blue concentration in the presence of oxygen (1) and in deaerated solutions (2). $[\text{ZnO}] = 1\times10^{-3}$ M, $[AgNO_3] = 1 \times 10^{-4}$ M. (b) The correlation between the rate of Ag(I) reduction and zinc oxide concentration. $[AgNO_3] = 1 \times 10^{-4}$ M, $[\text{MB}] = 1\times10^{-5}$ M.

this figure with oxidation potentials of the excited forms of MB shows that electron injection into ZnO nanoparticles is possible only with the participation of singlet excited state of MB. High rates of Ag(I) photoreduction in the presence of efficient quenchers of MB triplet state – molecular oxygen and phenylenediamine – also indicate on the participation of singlet-excited dye in the photoprocess. Due to very short lifetime of singlet-excited state of MB, the electron transfer to ZnO nanoparticles is possible only if the dye molecule is close to the surface of ZnO in the moment of light absorption. It was found that the langmuirian correlation (18) between the rate of Ag(I) photoreduction and MB concentration actually exists, confirming the participation of the absorbed dye in the photo process. Electrons, injected in ZnO nanoparticles, can then reduce MB molecules ($E^0(D/D^{\bullet\ -})$ $\sim$−0.2 V versus NHE (Lee & Mills, 2003)).

Redox-potential of the couple $Ag(I)/Ag^0_{atom}$ is −1.8 V versus NHE (Henglein, 1993). Hence, the energies of singlet and triplet excited states of MB are obviously insufficient for the transformation of Ag(I) into Ag^0_{atom}. This is apparently the reason why Ag(I) reduction has not been observed in the absence of ZnO nanoparticles. In the presence of ZnO nanocrystals, able to adsorb and concentrate silver ions, the photoreduction of Ag(I) by injected electrons can be substantially facilitated due to the formation of charged clusters, like Ag_2^+ (Henglein, 1993). Adsorption of atomic silver on the surface of ZnO can also results in partial compensation of uncoupled 4s-electron of silver atoms and considerable reduction of $E^0(Ag(I)/Ag^0_{atom})$. The growth of the photoreaction rate in the presence of NaOH (CH_3COONa) may be explained by the augmentation of the potential of ZnO conduction band due to the adsorption of OH^- on the surface of the semiconductor (Bahnemann, 1987). This effect does not impede the electron injection from the excited dye since the gap between E^1_{ox}(MB) and E_{CB}(ZnO) remains sufficiently large, but, at the same time, it facilitates reduction reactions with the participation of ZnO conduction band electrons.

Electron transfer from excited MB molecule to ZnO nanoparticle results in the formation of oxidized form of the dye $D^{\bullet+}$. This form can then oxidize 2-propanol ($E^0_{Ox} = -0.22$ V versus NHE), restoring ground state of the dye. Methyloxyethyl radicals, generated in this reaction ($E^0 = -1.8$ V versus NHE (Henglein, 1993)), can in turn reduce MB molecules. The following scheme summarizes the processes following the photoexcitation of the dye:

$$D + []_{ads} \rightarrow D_{ads} \tag{19}$$

$$Ag(I) + []_{ads} \rightarrow Ag(I)_{ads} \tag{20}$$

$$D_{ads} + h\nu \rightarrow D^1_{ads} \tag{21}$$

$$D^1_{ads} + ZnO \rightarrow (D^{+\bullet}_{ads}) + ZnO(e^-_{tr}) \tag{22}$$

$$D^{+\bullet}_{ads} + (CH_3)_2CHOH \rightarrow D_{ads} + (CH_3)_2C^{\bullet}OH + H^+ \tag{23}$$

$$(CH_3)_2C^{\bullet}OH + ZnO \rightarrow (CH_3)_2CO + ZnO(e^-_{tr}) + H^+ \tag{24}$$

$$D + ZnO(e^-_{tr}) \rightarrow D^{-\bullet} \tag{25}$$

$$D^{\bullet-} + ZnO(e^-_{tr}) \rightarrow D^{2-} \tag{26}$$

$$D(D^{\bullet-}) + (CH_3)_2C^{\bullet}OH \rightarrow D^{-\bullet}(D^{2-}) + (CH_3)_2CO + H^+ \tag{27}$$

$$2Ag(I)_{ads} + ZnO(e^-_{tr}) \rightarrow Ag^+_{2(ads)} \tag{28}$$

$$Ag^+_{2(ads)} + ZnO(e^-_{tr}) \rightarrow Ag^0_{2(ads)} \text{ and so on.} \tag{29}$$

where $[]_{ads}$ – is the adsorption site on the surface of ZnO nanoparticle.

Conclusions

We have discussed optical and some electrophysical properties of colloidal ZnO/Ag nanocomposites, forming in the result of photocatalytic reduction of $AgNO_3$ on the surface of ZnO nanoparticles in 2-propanolic solutions. We have focused mainly on the evolution of optical properties of the nanocomposite during its formation as well as on the kinetics of this process. Basic parameters of surface plasmon resonance bands have been calculated using Mie theory. It has been

found that good agreement between theoretical predictions of the maximum position and extinction coefficient of silver plasmon band and experimental results could be achieved only when the influence of ZnO on the optical properties of silver nanoparticles is taken into account. It has been shown that the hypsochromic shift of the maximum of silver plasmon band at the irradiation of ZnO/Ag particles is associated with the accumulation of the excess of electrons by composite nanoparticles. Electrons accumulation results in the equilibration between the Fermi energy of the nanocomposite and the conduction band edge of the semiconductor. The kinetics of photocatalytic Ag(I) reduction both in deaerated and in air-saturated solutions has been studied.

It has been shown that ZnO/Ag nanostructure can be formed at the irradiation with the visible light, absorbed by the sensitizer – methylene blue. The kinetics of the sensitized silver photoreduction has been thoroughly studied. It has been shown that the principal step of sensitization mechanism consists in the electron transfer between singlet excited methylene blue molecules and ZnO nanoparticles.

References

Albery J.W., 1985. Time-resolved photoredox reactions of colloidal CdS. J. Chem. Soc., Faraday Trans. 1(81), 1999–2007.

Bahnemann D.W., C. Kormann & M.R. Hoffmann, 1987. Preparation and characterization of quantum size zinc oxide: A detailed spectroscopic study. J. Phys. Chem. 91, 3789–3795.

Beydoun D., R. Amal, G. Low & S. McEvoy, 1999. Role of nanoparticles in photocatalysis. J. Nanoparticle Res. 1, 439–458.

Cozzoli P.D., E. Fanizza, R. Comparelli, M.L. Curri & A. Agostiano, 2004. Role of metal nanoparticles in TiO_2/Ag nanocomposite-based microheterogeneous photocatalysis. J. Phys. Chem. B 108, 9623–9630.

Doremus R.H., 1965. Optical properties of small silver particles. J. Chem. Phys. 42, 414–417.

Henglein A., 1993. Physicochemical properties of small metal particles in solution: ''Microelectrode'' reactions, chemisorption, composite metal particles, and atom-to-metal transition. J. Phys. Chem. 97, 5457–5471.

Henglein A., 1997. Nanoclusters of semiconductors and metals. Colloidal nanoparticles of semiconductors and metals: Electronic structure and processes. Ber. Bunsenges. Phys. Chem. 101, 1562–1569.

Henglein A., 1998. Colloidal silver nanoparticles: Photochemical preparation and interaction with O_2, CCl_4, and some metal ions. Chem. Mater. 10, 444–450.

Hoyer P. & H. Weller, 1995. Potential-dependent electron injection in nanoporous colloidal ZnO films. J. Phys. Chem. 99, 14096–14100.

James T.H., 1977. The Theory of Photographic Process. New York, London: Macmillan Publishing Co.

Kamat P.V., N.M. Dimitrijevic & A.J. Nozik, 1989. Dynamic Burstein-Moss shift in semiconductor colloids. J. Phys. Chem. 93, 2873–2875.

Khairutdinov R.F., 1998. Chemistry of semiconductor nanoparticles. Russ. Chem. Rev. 67, 125–128.

Kryukov A.I., S.Ya. Kuchmii & V.D. Pokhodenko, 2000. Energetics of the electronic processes in semiconductor photocatalytic systems. Theoret. Experim. Chem. 36, 69–87.

Kamat P.V., 2002. Photophysical, photochemical and photocatalytic aspects of metal nanoparticles. J. Phys. Chem. B 106, 7729–7744.

Kulak A.I., 1986. Electrochemistry of semiconductor heterostructures, Minsk, Universitetskoye.

Lee S.K. & A. Mills, 2003. Novel photochemistry of leucomethylene blue. Chem. Comm., 2366.

Liu C. & A.J. Bard, 1989. Effect of excess charge on band energetics (optical absorption edge and carrier redox potential) in small semiconductor particles. J. Phys. Chem. 93, 3232–3237.

Moelwyn-Hughes E.A., 1961. Physical Chemistry, Vol. II, London, New York, Paris: Pergamon Press.

Noack V., H. Weller & A. Eychmueller, 2002. Transport of a charge carrier packet in nanoparticulate ZnO electrodes. J. Phys. Chem. B 106, 384–394.

Patrick B. & P.V. Kamat, 1992. Photophysics and photochemistry of quantized ZnO colloids. J. Phys. Chem. 96, 1423–1427.

Pesika N.S., K.J. Stebe & P.C Searson, 2003. Relationship between absorbance spectra and particle size distributions for quantum-sized nanocrystals. J. Phys. Chem. B 107, 10412–10416.

Pileni M.P., 1998. Optical properties of nanosized particles dispersed in colloidal solutions or arranged in 2D or 3D superlattices. New J. Chem. 693–702.

Shim M. & P. Guyot-Sionnest, 2001. Organic-capped ZnO nanocrystals: Synthesis and *n*-type character. J. Am. Chem. Soc. 123, 11651–11654.

Skillman D.C. & C.R. Berry, 1968. Effect of particle shape on the spectral absorption of colloidal silver in gelatine. J. Chem. Phys. 48, 3297.

Stenzel O., 1999. Optical properties of noble metal clusters in ultra thin solid films. J. Cluster Sci. 10, 169–193.

Stroyuk A.L., A.I. Kryukov, S.Ya. Kuchmii & V.D. Pokhodenko, 2005a. Quantum size effects in the photonics of semiconductor nanoparticles. Theoret. Experim. Chem. 41, 67–91.

Stroyuk A.L., V.V. Shvalagin & S.Ya. Kuchmii, 2005b. Photochemical synthesis and optical properties of binary and ternary metal-semiconductor composites based on zinc oxide nanoparticles. J. Photochem. Photobiol. A: Chem. 173, 185–194.

Subramanian V., E.E. Wolf & P.V. Kamat, 2003. Green emission to probe photoinduced charging events in ZnO–Au nanoparticles. Charge distribution and Fermi-level equilibration. J. Phys. Chem. B 107, 7479–7485.

Tani T., L. Mädler & S.E. Pratsinis, 2002. Homogeneous ZnO nanoparticles by flame spray pyrolysis. J. Nanoparticle Res. 4, 337–343.

Terenin A.N., 1967. Photonics of Dye Molecules. Nauka: Leningrad.

Wang Y. & N. Herron, 1991. Nanometer-sized semiconductor clusters: Materials synthesis, quantum size effects and photophysical properties. J. Phys. Chem. 95, 525–532.

Wong E.M., P.G. Hoertz, C.J. Liang, B.-M. Shi, G.J. Meyer & P.C. Searson, 2001. Influence of organic capping on the growth kinetics of ZnO nanoparticles. Langmuir 17, 8362–8367.

Wood A., M. Giersig & P. Mulvaney, 2001. Fermi level equilibration in quantum dot – metal nanojunctions. J. Phys. Chem. B 105, 8810–8815.